Ocean Sci. Discuss., https://doi.org/10.5194/os-2018-80
Manuscript under review for journal Ocean Sci.
Discussion started: 11 September 2018

Ocean Science Discussions
Open Access

Genesis dynamics of the Angola-Benguela Frontal Zone

Shunya Koseki[1], **Hervé Giordani**[2], and **Katerina Goubanova**[3,4],

1. Geophysical Institute, University of Bergen, Bergen/Bjerknes Centre for Climate Research, Norway
2. Centre National de Recherches Météologiques, MÉTÉO-France, Toulouse, France
3. Centro de Estudios Avanzados en Zonas Áridas, La Serena, Chile
4. CECI/CERFACS-CNRS, Toulouse, France

Correspondence to Shunya Koseki

Email: Shunya.Koseki@gfi.uib.no

Address: Geophysical Institute, University of Bergen, Postboks 7803, 5020, Bergen, Norway

Ocean Sci. Discuss., https://doi.org/10.5194/os-2018-80
Manuscript under review for journal Ocean Sci.
Discussion started: 11 September 2018

Abstract

A diagnostic analysis of the climatological annual mean and seasonal cycle of the Angola Benguela Frontal Zone (ABFZ) is performed applying an ocean frontogenesis function (OFGF) to the ocean mixing layer (OML). The OFGF reveals that meridional confluence and the vertical tilting terms are the most dominant contributors to the frontogenesis of the ABFZ. The ABFZ shows a well-pronounced semi-annual cycle with two maximum (minimum) peaks in April-May and November-December (February-March and July-August). The development of the two maxima of frontogenesis is due to two different physical processes: enhanced tilting form March to April and the meridional confluence from September to October, respectively. The strong meridional confluence in September-October is closely related to the seasonal southward intrusion of tropical warm water to the ABFZ that seems to be associated with the development of the Angola Dome northwestern of the ABFZ. The strong tilting effect from March to April is attributed to the meridional gradient of vertical velocities whose effect is amplified in this period due to increasing stratification and shallow OML depth. The proposed OFGF can be viewed as a tool to diagnose the performance of CGCMs that generally fail in simulating realistically the position of the ABFZ, which leads to huge warm biases in the southeastern Atlantic.

Ocean Sci. Discuss., https://doi.org/10.5194/os-2018-80
Manuscript under review for journal Ocean Sci.
Discussion started: 11 September 2018

1. Introduction

The Angola-Benguela Frontal Zone (ABFZ, see Fig. 1), situated off the coast of Angola/Namibia, is a key oceanic feature in the southeastern Atlantic Ocean. The ABFZ separates the warm sea water of the Angola Current (e.g., Kopte et al., 2017) from the cold sea water associated with the Benguela Current/upwelling system (e.g., Mohrholz et al., 2004; Colberg and Reason, 2006; Veitch et al., 2006; Colberg and Resason, 2007; Fennel et al., 2012; Goubanova et al., 2013; Junker et al., 2015; Junker et al., 2017; Vizy et al., 2018). The ABFZ is characterized by smaller spatial extent and weaker SST gradient compared to the major oceanic fronts generated by the western boundary currents (Fig. 1). However, due to its near coastal location, the ABFZ plays important roles for the southern African continent, strongly impacting local marine ecosystem (e.g., Auel and Verheye, 2007; Chavez and Messié, 2009) and regional climate over the southern African Continent (Hirst and Hastenrath, 1983; Rouault et al. 2003; Hansingo and Reason, 2009; Manhique et al., 2015). In particular, the main model of interannual variability of SST in the ABFZ, so-called Benguela Niño/Niña (e.g., Florenchie et al., 2003; Rouault et al., 2017), influences the local rainfall along the southwestern African coast of Angola and Namibia (Rouault et al., 2003; Lutz et al., 2015) and tends to have a remote impact on rainfall activity over the southeastern African continent (e.g., Manhique et al., 2015).

The ABFZ region also poses one of the major challenges for the global climate modeling community. Most coupled general circulation models (CGCMs) exhibit a huge warm SST bias in the ABFZ (e.g., Zuidema et al., 2016) and fail to reproduce the realistic SST, its seasonal cycle and the right location of the ABFZ (e.g., Koseki et al., 2017). While Colberg and Reason (2006) and Giordani et al. (2011) concluded that the position of the ABFZ is controlled to a large extent by the local wind stress

Ocean Sci. Discuss., https://doi.org/10.5194/os-2018-80
Manuscript under review for journal Ocean Sci.
Discussion started: 11 September 2018

curl, Koseki et al. (2017) elucidated that the local wind stress curl bias in GCM contributes partly to the warm SST bias in the ABFZ via erroneous intrusion of tropical warm water, which is induced by the negative wind stress curl and enhanced Angola Current. In order to reduce this kind of model biases, one need to understand the processes of generation of the ABFZ.

Previous studies have focused mainly on SST variability at seasonal and interannual scales in the ABFZ and its impacts on regional climate are well-studied (e.g., Rouault et al., 2003; Lutz et al., 2015). To our knowledge, there are no works insightfully investigating dynamical and thermodynamical processes which generate and maintain the ABFZ and its seasonal cycle. A dynamical diagnosis for the SST front in the north of the Atlantic Cold Tongue (e.g., Hasternrath and Lamb, 1978; Giordani et al., 2013) was proposed by Giordani and Caniaux (2014, hereafter referred as GC2014). This frontogenetic function is, in general, adapted to explore sources of frontogenesis of atmospheric synoptic-scale cyclones at the extratropics (e. g., Keyser et al., 1988; Giordani and Caniaux, 2001). Using a frontogenetic function GC2014 showed clearly that the convergence associated with the northern South Equatorial Current and Guinea Current forces the SST-front intensity (frontogenetic effect) and mixed-layer turbulent flux destroys the SST-front (frontolytic effect) in climatology. Fundamentally, the frontogenetic function consists of three mechanical terms (confluence, shear and tilting) and two thermodynamical terms (diabatic heating and vertical mixing). Around the ABFZ, all these terms can be considered as contributors to the frontogenesis due to: (1) two opposite outstanding ocean current systems, the Angola and Benguela currents (confluence and shear). (2) strong coastal upwelling (tilting) associated with Benguela current; (3) one of the largest and more persistent stratocumulus cloud deck in the world (diabatic heating related to radiation)

Ocean Sci. Discuss., https://doi.org/10.5194/os-2018-80
Manuscript under review for journal Ocean Sci.
Discussion started: 11 September 2018

associated with the cold SST and subsidence due to St. Helena Anticyclone (e.g., Klein and Hartmann, 1993; Pfeifroth et al., 2012). So far, the relative roles of these different processes in the frontogenesis of the ABFZ still need to be investigated.

In this study, following the fundamental philosophy of GC2014, we attempt to understand the mechanisms responsible for the ABFZ development at seasonal scale based on a first-order estimation. We propose an ocean frontogenetic function in a different way from GC2014 (this study focuses on the ocean-mixed layer mean front). The structure of the remainder of this paper is as follows: Section 2 gives details of data set used in this study. In section 3, we derive the ocean frontogenetic function. Section 4 provides a description of the climatological state around the ABFZ. In section 5, we apply our diagnostic methodology to the ABFZ and determine the main terms of the frontogenetic function controlling its annual cycle. The associated processes are discussed in section 6. Finally we summarize and put some concluding remarks in section 7.

2. Data

For an overview of SST and its meridional gradient in the ABFZ and evaluation of reanalysis data, we employ the Optimum Interpolated Sea Surface Temperature (OISST, Reynolds et al., 2002) released by National Ocean and Atmosphere Association (NOAA) that has a quarter degree of horizontal resolution and daily temporal resolution from 1982 to 2010. For the 3-dimensional diagnostic analysis of the ABFZ, we utilize 1-hour forecast data of Climate Forecast System Reanalysis (CFSR, Saha et al., 2010) developed by the National Centers for Environmental Prediction (NCEP). The ocean component of this system is based on

Ocean Sci. Discuss., https://doi.org/10.5194/os-2018-80
Manuscript under review for journal Ocean Sci.
Discussion started: 11 September 2018

MOM version 4p0d (Griffies et al., 2004). This system provides 6-hourly data with a 0.5 degree horizontal resolution and 70 vertical layers for ocean. In this paper we will analyze daily-means. Data of sea water potential temperature (hereafter, referred to as temperature) is used for the analysis because sea water temperature and sea water potential temperature are almost identical in the upper ocean layers.

3. Ocean Frontogenesis Function

The ocean frontogenetic function (OFGF) is defined and applied to the ocean mixing layer (OML) in order to propose a dynamical diagnosis of the maintenance/generating process of the ABFZ. Following GC2014, we use the OFGF as a tool to unravel the Langrangian (pure) sources of the oceanic front. While there are plentiful numbers of literature investigating the ocean front dynamics (e.g., Dinniman and Rienecker, 1999), the concept of this OFGF has been hardly referred. The Lagrangian frontogenesis function, F, is defined as,

$$F \equiv \frac{d}{dt}\left(\frac{\partial \theta}{\partial y}\right) \qquad (3.1),$$

where, θ is the temperature. While the frontogenetic function is generally defined as the square of the horizontal gradient of the temperature (e.g., GC2014), our study employs only the meridional gradient of the temperature because the ABFZ SST-gradient is oriented South-North. The right hand side of Eq. 3.1 can be written as,

Ocean Sci. Discuss., https://doi.org/10.5194/os-2018-80
Manuscript under review for journal Ocean Sci.
Discussion started: 11 September 2018

$$
\begin{aligned}
\frac{d}{dt}\left(\frac{\partial\theta}{\partial y}\right) &= u\frac{\partial}{\partial x}\left(\frac{\partial\theta}{\partial y}\right) + v\frac{\partial}{\partial y}\left(\frac{\partial\theta}{\partial y}\right) + w\frac{\partial}{\partial z}\left(\frac{\partial\theta}{\partial y}\right) + \frac{\partial}{\partial t}\left(\frac{\partial\theta}{\partial y}\right) \\
&= -\frac{\partial u}{\partial y}\frac{\partial\theta}{\partial x} - \frac{\partial v}{\partial y}\frac{\partial\theta}{\partial y} - \frac{\partial w}{\partial y}\frac{\partial\theta}{\partial z} + \frac{\partial}{\partial y}\left(\frac{\partial\theta}{\partial t} + u\frac{\partial\theta}{\partial x} + v\frac{\partial\theta}{\partial y} + w\frac{\partial\theta}{\partial z}\right) \\
&= -\frac{\partial u}{\partial y}\frac{\partial\theta}{\partial x} - \frac{\partial v}{\partial y}\frac{\partial\theta}{\partial y} - \frac{\partial w}{\partial y}\frac{\partial\theta}{\partial z} + \frac{\partial}{\partial y}\left(\frac{d\theta}{dt}\right)
\end{aligned}
\qquad (3.2)
$$

Here, u, v, and w denote the current velocity and we use the relation between Lagrangian and Eulerian differentiations. Equation 3.2 describes the processes that act to generate/destroy the ocean front. The terms $-\frac{\partial u}{\partial y}\frac{\partial\theta}{\partial x}$, $-\frac{\partial v}{\partial y}\frac{\partial\theta}{\partial y}$, and $-\frac{\partial w}{\partial y}\frac{\partial\theta}{\partial z}$ are the contributions due to the mechanical processes: shear, convergence and tilting, respectively. The shear term represents conversion of the zonal temperature gradient into meridional gradient by zonal current shear. The convergence term represents strengthening/weakening of the meridional temperature gradient by convergence/divergence of meridional current. The tilting term represents conversion of the vertical stratification into meridional gradient by meridional shear of vertical velocity.

The fourth term is a thermodynamical term due to exchange heat associated with the turbulent heat flux. This term can be expressed as,

$$
\frac{\partial}{\partial y}\left(\frac{d\theta}{dt}\right) = \frac{\partial}{\partial y}\left(-\frac{\partial\overline{w'\theta'}}{\partial z}\right) \qquad (3.3).
$$

The contribution due to the second order horizontal diffusion is ignored for simplicity.

Since within the OML the temperature is fairly uniform (cf. Fig. 2 to compare the SST and OML-averaged temperature), we consider the OFGF with the mixed-

Ocean Sci. Discuss., https://doi.org/10.5194/os-2018-80
Manuscript under review for journal Ocean Sci.
Discussion started: 11 September 2018

Ocean Science
Discussions
Open Access

layer mean quantities. With the approximation that temperature is independent of the depth in the OML (Kazmin and Rienecker, 1996), Eq. 3.2 can be expressed as,

$$\frac{d}{dt}\left(\frac{\partial \theta_{oml}}{\partial y}\right) = -\frac{\partial u_{oml}}{\partial y}\frac{\partial \theta_{oml}}{\partial x} - \frac{\partial v_{oml}}{\partial y}\frac{\partial \theta_{oml}}{\partial y} - \frac{\partial w_b}{\partial y}\frac{\Delta\theta}{D} + \frac{\partial}{\partial y}\left(\frac{Q_s + Q_b}{\rho C_p D}\right) \quad (3,4),$$

where, the subscript of *oml* indicates the OML-mean quantity. Although the horizontal velocity is a function of depth even in the OML, the horizontal mechanical terms in Eq. 3.4 can be written in terms of OML-mean quantities because the production remains linear relation as long as the temperature is independent of depth in the OML. w_b, $\Delta\theta$ and D represent the vertical velocity, the temperature jump at the bottom of the OML and the OML depth. We use constant values for sea water density, ρ (1000 kg/m^3) and isobaric specific heat of sea water, C_p (4200 Jkg^{-1}K^{-1}). The vertical mixing term is replaced with Q_s and Q_b, where Q_s is the surface net heat flux at the top of OML (downward is positive in this study) and Q_b represents the vertical mixing at the bottom of the OML, i.e., in the thermocline. We assume that there is no penetration of shortwave radiation beyond the OML to deeper ocean layers. Because the vertical mixing term expressed by Q_b is a higher-order term, it is expressed as an additional term; it will be not addressed explicitly in this study.

While Eq. 3.4 is Langrangian form of the OFGF, the equation can be also expressed in Eulerian form as below:

$$\frac{\partial}{\partial t}\left(\frac{\partial \theta_{oml}}{\partial y}\right) = \underbrace{-\frac{\partial u_{oml}}{\partial y}\frac{\partial \theta_{oml}}{\partial x}}_{\text{SHER}} \underbrace{-\frac{\partial v_{oml}}{\partial y}\frac{\partial \theta_{oml}}{\partial y}}_{\text{CONF}} \underbrace{-\frac{\partial w_b}{\partial y}\frac{\Delta\theta}{D}}_{\text{TILT}} + \underbrace{\frac{\partial}{\partial y}\left(\frac{Q_s}{\rho C_p D}\right)}_{\text{SFLX}} + \underbrace{\text{residual}}_{\text{RESD}} \quad (3.5).$$

Ocean Sci. Discuss., https://doi.org/10.5194/os-2018-80
Manuscript under review for journal Ocean Sci.
Discussion started: 11 September 2018

The contribution due to the vertical mixing Q_b, is estimated as residual of Eq. (3.5). Along with the vertical mixing, the residual term also includes the horizontal and vertical advection of the $\partial\theta_{oml} / \partial y$ which are not related to Lagrangian sources of the frontogenesis either. In the reminder of this paper, the shear term will be referred to as SHER, the confluence as CONF, the tilting as TILT, the thermodynamic term as SFLX and the residual as RESD.

Note that basically, our climatology is a 29-years mean from 1982 to 2010. However, some years do not have OML data at some grid points around the coastal region. For these grid points, we make the climatology only for available years. For example, the smallest number in the focusing ABFZ is 16 years at 16.25 °S.

4. Overview of the ABFZ and its Seasonal Cycle in CFSR data

Before the dynamical diagnosis is performed, we provide a brief overview of the main feature of the ABFZ. The maximum of the ABFZ (up to 1.4 °C/100km) is located at 16 °S just near the coast (Fig.1b). Figure 2a shows a seasonal cycle of the temperature and its meridional gradient obtained from the satellite product OISST. The core (SST meridional gradient exceeds 1.0 °C/100km) of the ABFZ always lies between 17 °S and 15 °S. At seasonal scale, the location of the ABFZ exhibits rather a weak variability compared to strong interannual variability associated with the Bengulea Niños that push the ABFZ southward due to the southward intrusion of tropical warm water (e.g., Gammelsrød et al. 1998; Veitch et al., 2006; Rouault et al., 2017). For instance, Rouault et al. (2017) shows that during Benguela Niño 2010-2011 the ABFZ displaced southward as far as 20°S. The intensity of the ABFZ shows a pronounced seasonal cycle: there are two peaks of the strength in April-May and

Ocean Sci. Discuss., https://doi.org/10.5194/os-2018-80
Manuscript under review for journal Ocean Sci.
Discussion started: 11 September 2018

November-to-December, respectively. The semi-annual cycle of the ABFZ will be examined in more details in the following sections. Figures 2b and c evidence that the CFSR reanalysis reproduces realistically the annual cycle of the ABFZ, and that the annual cycle of the corresponding OML-mean temperature meridional gradient is representative of the annual cycle of the SST meridional gradient in terms of both timing and intensity of the two annual peaks. This latter result justifies our approach to diagnose the frontogenesis of the ABFZ with the OML-mean quantities.

5. Dynamical Diagnosis on the ABFZ

In this section, we investigate the frontogenesis of the ABFZ diagnostically applying the OFGF described in Section 3. Figure 3 illustrates the climatological annual-mean oceanic dynamical fields. The southwestward Angola and northwestward Benguela alongshore currents collide just south of the ABFZ. Seaward from the ABFZ, a strong westward current is detected. Intense upwelling (vertical velocity at the bottom of OML exceed 0.18 m/day) is generated along the coast in the Benguela Current region. A local maximum of upwelling in the ABFZ (approximately 17 °S) corresponds to one of the most vigorous upwelling cells in the region, namely Cape Frio cell (Lutjeharms and Meeuwis, 1987). Note also a relatively weak downwelling cell (vertical velocity down to -0.06 m/day) just seaward from the Cape Frio upwelling cell.

5.1 Annual-mean state

Ocean Sci. Discuss., https://doi.org/10.5194/os-2018-80
Manuscript under review for journal Ocean Sci.
Discussion started: 11 September 2018

Figure 4 presents the annual-mean climatology of the 5 forcing/source terms of the OFGF superimposing the meridional gradient of the OML-mean temperature. SHER works frontolytically (destroying the front, about -2 °C/100 km×10^{-7} s^{-1}) in the most parts of the ABFZ except just near the coast at 17 °S, although its frontogenetic (generating front) contribution here is rather weak (less than 2 °C/100 km×10^{-7} s^{-1}). CONF has on average an intense frontogenetic contribution to the ABFZ (up to 5 °C/100 km×10^{-7} s^{-1}), especially offshore around 16 °S where the ABFZ is centered (Fig. 2). The frontogenetic effect of CONF is consistent with GC2014 (the frontogenesis of the SST front associated with the equatorial Atlantic cold tongue is due to the confluence of northern South Equatorial Current and Guinea Current) and can be expected because the warm and cold currents meet around the ABFZ. Note however a small zone just near the coast at 16 °S where the CONF is frontolytic. This local frontolytic contribution is overcompensated by a strong frontogesis due to TILT (more than 5 °C/100 km×10^{-7} s^{-1} on average in the ABFZ core). An elongated frontogentic zone associated with TILT is found along the Angolan coast from 17°S to 11°S and corresponds to the upwelling tongue observed in the Angola current region (Fig.3). On the other hand, TILT is frontolytic off the ABFZ (at 17°S, 11°E) where the downwelling is dominant as shown in Fig.3. The role of the upwelling in the ABFZ development will be analyzed in more details in the Section 6.2.

In addition to the mechanical terms, the thermodynamical components also show some influences on the ABFZ. SFLX works frontogenetically just near the coast at 16°S and frontolytically south and north from the core of the ABFZ, although its contribution is almost negligible compared to the mechanical contribution. RESD is estimated by,

Ocean Sci. Discuss., https://doi.org/10.5194/os-2018-80
Manuscript under review for journal Ocean Sci.
Discussion started: 11 September 2018

$$\mathrm{RESD}=\frac{\partial u_{oml}}{\partial y}\frac{\partial \theta_{oml}}{\partial x}+\frac{\partial v_{oml}}{\partial y}\frac{\partial \theta_{oml}}{\partial y}+\frac{\partial w_b}{\partial y}\frac{\Delta\theta}{D}-\frac{\partial}{\partial y}\left(\frac{Q_s}{\rho C_p D}\right) \quad (5.1)$$

where, we assume that there is no local temporal tendency of the front, $(\partial\theta_{oml}/\partial y)/\partial t$ so that Eq. (3.5) can be closed. One annual time scale this approximation is robust. On average in the core of the ABFZ, RESD shows a strong frontolytic contribution around the core of the ABFZ (Fig. 4e). On the other hand, frontogenesis is located in the southern part of the ABFZ. This may be due to, at least, to vertical mixing at the base of the OML accounted for in RESD. According to GC2014, the turbulent mixing (surface and thermocline heat fluxes) is frontolytic in the equatorial front.

5.2 Seasonal Cycle

In the preceding subsection, we have shown that in terms of climatological annual-mean terms CONF and TILT of the OFGF are the main drivers for the ABFZ generation. Next, we analyze the annual cycle of the ABFZ and its relationship to the seasonal variations of the OFGF terms. Note that Eq. 3.5 implies $\pi/2$ out of phase between the OFGF and temperature meridional gradient. This means that for a semi-annual oscillation the temperature meridional gradient should lead the OFGF by approximately 1 and half months.

Figure 5a illustrates the box-mean (10 °E-12 °E and 17 °S-15 °S) temporal series of the meridional gradient of temperature obtained from satellite and reanalysis products (the time series is smoothed by a 11-days-mean moving filter). There is an obvious semi-annual cycle of the ABFZ with maxima in April-May and in November-December, respectively, and minima in February-March and July-August, respectively (see also Fig.2). The first maximum develops rapidly (during 2 month, from March to April) whereas the development of the second maximum is somewhat slower (3 months, from August to October). Figure 5a also evidences that CFSR reproduces realistically the semi-annual cycle, although the magnitudes of the CFSR meridional SST gradient are generally slightly stronger with respect to OISST.

We further analyze the seasonal cycle of the OFGF terms. Similarly to the climatological state in Fig. 4, the contributions of SHER and SFLX are relatively small and do not seem to be responsible for either of the two peaks in the ABFZ annual cycle (not shown). Figure 5b shows the seasonal variations of TILT, CONF, and RESD averaged over the same box as the temperature gradients in Fig. 5a. For estimation of seasonal variation of RESD, the tendency of the meridional gradient is calculated as,

$$\frac{\partial}{\partial t}\left(\frac{\partial \theta_{oml}(t)}{\partial y}\right) = \frac{\dfrac{\partial \theta_{oml}(t+1)}{\partial y} - \dfrac{\partial \theta_{oml}(t-1)}{\partial y}}{2\times \mathrm{Day}}, \quad (5.2)$$

where, t denotes each time step, in this case, daily. With this tendency at each day, RESD(t) is estimated by

$$\mathrm{RESD}(t) = \frac{\partial}{\partial t}\left(\frac{\partial \theta_{oml}(t)}{\partial y}\right) - \mathrm{SHER}(t) - \mathrm{CONF}(t) - \mathrm{TILT}(t) - \mathrm{SFLX}(t).$$

From the middle of November to February, the box-averaged CONF is modestly negative, which is due to the frontolytic effect adjacent to the Angolan coast as shown in Fig. 4b (however, CONF is frontogenetic off the ABFZ). The contribution of CONF becomes positive from March, although its frontogenetic contribution is relatively weak (< 1.0 °C/100 km×10^{-7} s^{-1}) until July. From the end of

July CONF starts to increase and reaches its maximum (3.0 °C/100 km×10^{-7} s^{-1}) in the end of August. The frontogenetic contribution of CONF remains strong until the beginning of October but then rapidly decrease to become frontolytic in November.

The contribution of TILT to the ABFZ seasonal cycle is almost always frontogenetic. Close to zero in January, TILT is enhanced from February and reaches its maximum value (3.0 °C/100 km×10^{-7} s^{-1}) in March-April. In May-June, the frontogenetic effect of TILT gradually decreases (down to 1.0 °C/100 km×10^{-7} s^{-1}) until December. The maxima in TILT and CONF correspond to the two periods of development of the ABFZ at seasonal scale: from March to April and from August to October, respectively (Fig. 5a). This suggests that the two peaks of the ABFZ are associated with two different mechanical terms and thus are due to two different physical processes. On the other hand, the two periods of decay of the ABFZ are consistent with the periods of weak frontogenetic and/or frontolytic contributions of both TILT and CONF, in December-February and June-July, respectively.

In addition, RESD is almost always frontolytic with a relatively large oscillation (0.0 to -5.0 °C/100 km×10^{-7} s^{-1}) as shown in Fig.5b. In particular, the frontolytic effect due to RESD is stably strong (around -3.0 °C/100 km×10^{-7} s^{-1}) from May to August when the ABFZ becomes weakened and frontogenetic effects due to CONF and TILT are relatively weak (Figs. 5a and b). Conversely as TILT and CONF, RESD does not exhibit a clear signal of semi-annual cycle, but rather an annual-cycle. We thus can conclude that in terms of a first-order estimation, the semi-annual cycle of the ABFZ is explained by the combination of TILT and CONF.

6. Discussion

The previous section showed that the two periods of development of the ABFZ in March-April and August-October were due to a large extent to the contribution of TILT and CONF, respectively. In this section, we investigate what components are responsible for the corresponding peaks in TILT and CONF.

6.1 Meridional Confluence

CONF represents changes in the meridional temperature gradient associated with ocean dynamics of convergence/divergence of meridional current, $\partial v_{oml} / \partial y$. Figure 6a presents the annual cycle of $\partial v_{oml} / \partial y$ averaged over the ABFZ that shows a mirror image of the time series of CONF (Fig. 5). In the ABFZ, the meridional current is almost always convergent except for weak divergence from November to January. The convergence of the meridional current is maximum from August to mid-October (up to -3.0×10^{-7} s^{-1}) and is rapidly weakened during November. The seasonal fluctuations in the convergence are associated with changes in intensity and meridional extension of the southward Angola Current and northward Benguela Current that meet in the ABFZ. Figure 6b illustrates the annual cycle of OML-mean meridional current and meridional component of geostrophic current estimated from sea surface height (SSH) at 15 °S (north of the core of the ABFZ) and 17 °S (south of the core of the ABFZ) averaged between 10 °E and 12 °E. At 15 °S the OML-mean meridional current is southward all year round, except the beginning of May when a weak northward flow is observed. The maximum southward meridional velocity occurs in October (-0.12m/s). At 17 °S the OML-mean meridional current is northward in March-June and shows a bi-annual peak of southward current in January-to-mid-February and October indicating intrusion of tropical warm water to

Ocean Sci. Discuss., https://doi.org/10.5194/os-2018-80
Manuscript under review for journal Ocean Sci.
Discussion started: 11 September 2018

the ABFZ (e.g., Rouault, 2012). Figure 6b clearly evidences that the region between 17 °S and 15 °S is expected to be convergent. The most convergent period is in September-October when the CONF contribution to frontogenesis is the largest as shown in Fig. 5b. Another relatively strong convergent period is from April to June when the meridional current is rather northward at 17 °S and close to zero at 15° S. The period of weak convergence/divergence, form December to February, corresponds to frontolytic contribution of CONF (Figs.5b). Figure 6b evidences that the OML-mean meridional current can be explained, to a large extent, by the geostrophic surface current.

The spatial distributions of the climatological monthly mean SSH and surface geostrophic current in January, April, and September are shown in Figure 7. Two local minima of SSH are observed: one along the coast in the Benguela system and one west of the ABFZ (centered at 14 °S and 6 °E). The latter is associated with the Angola Dome (e.g., Doi et al. 2007) and a strong cyclonic geostrophic flow reaching the ABFZ. The geostrophic current generally generates the convergence in the ABFZ (Fig. 6a). However, in January an intense divergence is generated due to the strong southward ageostrophic current along the coast (Fig. 7a). In April, when CONF is modestly frontogenetic (Fig.5b), the Angola Dome and associated geostrophic flow are diminished (Fig. 7b) and a main source of convergence can thus be attributed to the northward Benguela Current which penetrates into the ABFZ as far as up to 16 °S. In September, whereas the low SSH sits in the south of the ABFZ as in April, the Angola Dome is significantly developed to induce a strong geostrophic current resulting in a strong southward Angola Current intruding into the ABFZ along the Angolan coast. The northward Benguela Current is relatively weak in September compared to that in April. Thus, the maximum CONF in September is due to the strong southward Angola Current.

6.2 Tilting

TILT is the second main contributor to generate the ABFZ especially in March-to-May as shown in Figs. 4 and 5. In a first approximation TILT results from the meridional gradient of vertical motion $\partial w_b / \partial y$ convoluted with the thermocline stratification (e.g., Eq.3.5). Here, we explore more details of upwelling in the ABFZ. The annual cycle of these two components averaged over the box [12 °E-10 °E] and [17 °S-15 °S] (Fig.8) points out that $\partial w_b / \partial y$ and the stratification is negative and positive, respectively, from January to August. This configuration leads to frontogenesis through the TILT term (Fig. 5b). From August to December, $\partial w_b / \partial y$ changes sign and the stratification becomes weaker; that explains why the TILT term is frontolytic (especially in September) and its magnitude is weaker compared to January-August because of a weaker stratification. Negative $\partial w_b / \partial y$ can be seen in both March to April and August to September around the ABFZ in Figs. S1a and b, but positive $\partial w_b / \partial y$ are also generated around the ABFZ more in August-September than in March-April.

The OML depth has extrema in August to September (around 100 m) and from January to April (around 20 m) indicating the seasonal cycle of solar insolation forcing. Also the intensity of the thermocline shows a strong stratification from March to May (2°C) and weak stratification from September to November (1.2°C). From March to May TILT is the most dominant frontogenetic source because the OML is

Ocean Sci. Discuss., https://doi.org/10.5194/os-2018-80
Manuscript under review for journal Ocean Sci.
Discussion started: 11 September 2018

the shallowest (20-30m), the stratification is the strongest (up to 2.0K) and the shear of vertical velocity $\partial w_b / \partial y$ is strongly negative. The shallow OML and strong stratification can amplify the tilting effect due to $\partial w_b / \partial y$. Conversely, TILT is weakly frontolytic from August to September when the OML-depth is deepened (~100m), the stratification is weak (1.2K) and $\partial w_b / \partial y$ is positive. Fig.S1c and d shows the differences in OML depth and ocean stratification between March-April and August-September. Shallower OML and stronger stratification can be seen everywhere around the ABFZ. Therefore, ~~the~~ effects of both positive and negative $\partial w_b / \partial y$ are reduced and consequently, contribution of TILT is quite weak in August to September (Fig. 5b).

7. Concluding Remarks

In this study we investigated the processes controlling the ABFZ evolution based on a first-order estimation of an ocean frontogenetic function (OFGF) applied to the ocean mixing layer (OML) derived from the CFSR reanalysis. The OFGF represents the temporal evolution of the meridional mixed-layer temperature gradient and contains three mechanical terms (shear, convergence and tilting) and one thermodynamical term. The residual term accounts for higher-order terms, associated in particular with vertical mixing and horizontal/vertical advections of the meridional temperature gradient. An analysis of the annual mean OFGF suggests that the confluence effect (CONF) due to southward Angola Current (warm) and northward Benguela Current (cold) is dominantly frontogenetic over the offshore part of the ABFZ, although it has a local frontolytic effect just near the coast at 16ºS. The tilting effect (TILT) related to the coastal upwelling regime is another main contributor to frontogenesis..The contributions of the shear (SHER) and surface heat flux (SFLX) terms, are rather negligible, while the residual (RESD) represents a main frontolytic source.

Seasonal evolution of the ABFZ has a well-pronounced semi-annual cycle with two maxima, in April-May and November-December, and two minima, in February-March and July-August. We showed that the two maxima of the ABFZ were associated with two different mechanical terms and due to two different physical processes. The development of the first ABFZ maximum during March-April is mainly explained by the strong contribution of TILT to frontogenesis, while the development of the second ABFZ maximum during September-October is due to the frontogenetic contribution of CONF. TILT is associated with the merdional gradient of the vertical velocity. The annual maximum of TILT in March-April is due to a large extent to the combination of the maximum stratification ($\Delta\theta$), shallow OML depth (D) and negative $\partial w_b / \partial y$ during this period. Indeed, in OFGF formulation the ratio $\frac{\Delta\theta}{D}$ represents the efficiency by which the meridional gradient of the coastal upwelling velocity can lead to the change of the ABFZ intensity. Although the OML depth also modulates the surface heat flux contribution to the OFGF, the thermodynamical term does not show any significant impact on the development of the ABFZ maximum in March-April. On the other hand, the importance of the OML depth for the thermodynamical term was suggested for frontogenesis in a SST front associated with western boundary current (Tozuka and Cronin, 2014; Tozuka et al., 2018). The annual maximum of CONF in September-October is related to an intensified southward Angola current that seems to be induced by a cyclonic geostrophic flow associated with the development of the Angola Dome (e.g., Doi et al., 2007). A relatively smaller contribution of CONF to frontogenesis is also observed in April and is due to the intrusion of the northward Benguela Current to the ABFZ during this period.

Most CGCMs fail to reproduce realistic SST field and ABFZ location. Among other causes, this can be due to a poor representation of regional climate variables in CGCMs, such as upwelling favorable wind, near-coastal wind curl and wind drop off, alongshore stratification and OML depth (e.g., Xu et al., 2014; Koseki et al., 2018; Goubanova et al., 2018), that impact directly the two main frontogenesis terms, CONF and TILT. The OFGF proposed in the present study can be thus an appropriate tool to diagnose the performance of CGCMs in the ABFZ and more generally in frontal zones. This study shows that diagnosis developed for mesoscale studies are valuable for climate studies and can help to identify the origin of biases which affect OGCMs. Effects of the turbulent mixing at the mixed-layer base on frontogenesis were accounted by the residual of the frontogenetic function. This is the main limitation of this study because diapycnal mixing is often an important term of the oceanic upper-layers heat budget which is tightly coupled with vertical motions (Giordani et al., 2013). A more comprehensive understanding of this term would be valuable to estimate the performance of CGCMs in the ABFZ and more generally in coastal upwelling zones.

Acknowledgement

We greatly appreciate Dr. Kunihiro Aoki in the University of Tokyo for his constructive discussion in the beginning of stage of this study. We also thank to Dr.

Guy Caniaux in MÉTÉO-France for their helpful discussions. We utilized the versions of 2012Rb of MATLAB software package provided by The MathWorks, Inc., (http://www.mathworks.com) and Grid Analysis and Display System (GrADS, http://www.iges.org/grads/) to compute each dataset and create figures. The research leading to these results received funding from the EU FP7/2007-2013 under grant agreement to no. 603521 (EU-PREFACE).

Reference

Auel, H., and Verheye, H. M.: Hypoxia tolerance in the copepod Calanoides carinatus and the effect of an intermediate oxygen minimum layer on copecod vertical distribution in the northern Bengulea Current upwelling system and the Angola-Benguela Front. *J. Exp. Mar. Bio. Eco*., **352**, 234-243, doi:10.1026/j.jembe.2007.07.020, 2007.

Chavez, F. P., and Messié, M.: A comparison of eastern boundary upwelling ecosystem. *Prog. Oceanogr*., **83** (1-4), 80-96 (Dec, http://www.sciencedirect.com/science/article/pii/S0079661109000998, 2009.

Chelton, D.B., and Xie, S.-P.: Coupled ocean-atmosphere interaction at ocean mesoscales. *Oceanography*, **23(4)**, 52-69, doi:10.5670/oceanog.2010.05, 2010

Chen, Z., Yan, X.-H., Jp, Y.-H., Jiang, L., and Jiang, Y.: A study of Bengulea upwelling system using different upwelling indices derived from remotely sensed data.

Continental Shelf Research, **45**, 27-33, 2012.

Colberg, F., and Reason, C. J. C.: A model study of the Angola Benguela Frontal Zone: Sensitivity to atmospheric forcing. *Geophys. Res. Lett*., **33**, L19608, doi:10.1029/2006GL027463, 2006.

Colberg, F., and Reason, C. J. C.: A model investigation of internal variability in the Angola Benguela Forntal Zone. *J. Geophys. Res*., **112**, C07008, doi:10.1029/2006JC003920, 2007.

Dinniman, M. S., and Rienecker, M. M.: Frontogenesis in the North Pacific Ocean Frontal Zones-A Numerical Simulation. *J. Phy. Oceanogra*., **29**, 537-559, 1999.

Doi, T., T. Tozuka, Sasaki, H., Masumoto, Y., and T. Yamagata, T.: Seasonal and interannual variations of oceanic conditions in the Angola Dome. *J. Phys. Oceanogr*., **37**, 2698-2713, doi:10.1175/2007JPO3552.1, 2007.

Fennel, W., Junker, T., Schmidt, M., and Mohrholz, V.: Response of the Benguela upwelling system to spatial variations in the wind stress. *Continental Shelf Research*, **45**, 65-77, 2012.

Florenchie, P., Lutjeharms, J. E., Reason, C. J. C., Masson, S., and Rouault, M.: The source of Benguela Ninos in the South Atlantic Ocean. *Geophys. Res. Lett*., **30**, doi:10.1029/2003GL017172, 2003.

Gammelsrød, T., Bartholomae, C. H., Boyer, D. C., Filipe, V. L. L., and O'Toole, M. J.: Intrusion of warm surface water along the Angolan-Namibian coast in

Ocean Sci. Discuss., https://doi.org/10.5194/os-2018-80
Manuscript under review for journal Ocean Sci.
Discussion started: 11 September 2018

February-March 1995: the 1995 Benguela Nino. *South African Journal of Marine Science*, **19:1**, 41-56, doi:10.2989/025776198784126719, 1998.

Giordani, H., and Caniaux, G.: Sensitivity of cyclogenesis to sea surface temperature in the Northwestern Atlantic. *Mon. Wea. Rev.*, **129**(6), 1273-1295, 2001.

Giordani, H., and Caniaux, G.: Diagnosing vertical motion in the Equatorial Atlanitc. *Ocean Dynamics*, **61**(12), doi:10.1007/s10236-01—0467-7, 2012.

Giordani, H., Caniaux, G., and Voldoire, A.: Intraseasonal mixed-layer heat budget in the equatorial Atlantic during the cold tongue development 2006. *J. Geophys. Res*., **118**, 650-671, doi:10.1029/2012JC008280, 2013.

Giordani, H., and Caniaux, G.: Lagrangian sources of frontogenesis in the equatorial Atlantic front, *Clim. Dyn*., doi:10.1007/s00382-014-2293-3, 2014.

Goubanova, K., Illig, S., Machu, E., Garcon, V., and Dewitte, B.: SST subseasonal variability in the central Benguela upwelling system as inferred from satellite observation (1999-2009). *J. Geophys. Res*., **118**, 4092-4110, doi:10.1002/jgrc.20287, 2013.

Goubanova, K., Sanchez.Gomez, E., Frauen, C., and Voldoire A.: Role of remote and local wind stress forcing in the development of the warm SST errors in the southeastern tropical Atlantic in a coupled high-resolution seasonal hindcast, *Clim. Dyn*., doi:10.1007/s00382-018-197-0, 2018.

Ocean Sci. Discuss., https://doi.org/10.5194/os-2018-80
Manuscript under review for journal Ocean Sci.
Discussion started: 11 September 2018

Griffies, S. M., Harrison, M. J., Pacanowski, R. C., and Rosati, A.: Technical guide to MOM4. GFDL Ocean Group Technical Report No.5, 337 pp. [Available online at www.gfdl.noaa.gov/-fms], 2004.

Hanshingo, K., and Reason, C. J. C.: Modelling the atmospheric response over southern Africa to SST forcing in the southeast tropical Atlantic and southwest subtropical Indian Oceans. *Int. J. Climatol*., **29**, 1001-1012, doi:10.1002/joc.1919, 2009.

Hastenrath, S. and Lamb, P.: On the dynamics and climatology of surface flow over the equatorial oceans. *Tellus*, **30**, 436-448, 1978.

Hirst, A. C., and Hastenrath, S.: Atmopshere-Ocean Mechanisms of Climate Anomalies in the Angola-Tropical Atlantic Sector. *J. Phys. Oceanogr*., **13**, 1146-1157, doi:http://dx.doi.org/10.1175/1520-0485(1983)013<1146:AOMOCA>2.0.CO;2, 1983.

Junker, T., M. Schmidt, and Mohrholz, V.: The relation of wind stress curl and meridional transport in the Benguela upwelling system. *J. Marine. Res*., **143**, 1-6, 2015

Junker, T., Mohrholz, V., Siegfired, L., and van der Plas, A.: Seasonal to interannual variability of water mass characteristics and current on the Namibian shelf. *J. Mar. Syst*., **165**, 36-46, doi:10.1016/j.jmarsys.2016.09.003, 2017.

Kazmin, A. S., and Rienecker, M. M.: Variability and forntogenesis in the large-scale oceanic frontal zones. *J. Geophys. Res*., **101**, 907-921, 1996.

Keyser, D., Reeder, M. J., and Reed, R. J.: A Generalization of Petterssens's Frontogenesis Function and Its Relation to the Forcing of Vertical Motion. *Mon. Wea. Rev*., 116, 762-780, 1988.

Klein S. A., and Hartmann, D. L.: The Seasonal Cycle of Low Stratiform Clouds. *J. Climate*, **6**, 1587-1606, 1993.

Koseki, S., Keenlyside, N., Demissie, T., Toniazzo, T., Counillon, F., Bethke, I., Ilicak, M., and Shen, M.-L.: Causes of the large warm SST bias in the Angola-Benguela Frontal Zone in the Norwegian Earth System Model. *Clim. Dyn*., **50**, 4651-4670, doi:10.1007/s00382-017-3896-2, 2018.

Kopte, R, Brandt, P., Dengler, M., Tchipalanga, P. C. M., Macueria, M., and Ostrowski, M. : The Angola Current: Flow and hydrographic characteristic as observed at 11°S. *J. Geophys. Res. Oceans*, **122**, 1177-1189, doi:10.1002/2016JC012374, 2017.

Lütjeharms, J. E. R., and Meeuwis, J. M.: The extent and variability of south-east Atlantic upwelling, in the Benguela and comparable ecosystem, *S. Afr. J. Mar. Sci*., **5** , 1987.

Lutz, K., Jacobeit, J., and Rathmann, J.: Atlantic warm and cold water events and impact on African west coast precipitation. *Int. J. Climatol*., **35**, 128-141, doi:10.10002/joc.3969, 2015.

Manhique, A.J., Reason, C. J. C., Silinto, B., Zucula, J., Raiva, I., Congolo, F., and Mavume, A. F.: Extreme rainfall and floods in southern Africa in January 2013 and associated circulation patterns. *Nat., Hazards*, **77**, 679-691, doi:10.1007/s11069-015-1616-y, 2015.

Mohrholz, V., Schmidt, M., Lutjeharms, J. R. E., and John, H.-C.H.: Space-time behavior of the Angola-Benguela Frontal Zone during the Benguela Nino of April 1999. *Int. J. Remote Sensing*, **25**, 1337-1400, doi:10.1080/01431160310001592265, 2004.

Patricola, C. M., and Chang, P.: Structure and dynamics of the Benguela low-level coast jet. *Clim. Dyn*., doi:10.1007/s00382-016-3479-7, 2016.

Pfeifroth, U., Hollmann, R., and Ahrens, B.: Cloud Cover Diurnal Cycles in Satellite Data and Regional Climate Model Simulations. *Meteorologishe Zeitschrift*, **21**, 551-560, 2012.

Risien, C. M., and Chelton, D. B.: A global climatology of surface wind and wind stress fields from 8 years of QuikSCAT scatterometer data. *J. Phy. Oceano*., **38**, 2379-2413, 2008.

Rouault, M., Florenchie, P., Fauchereau, N., and Reason, C. J. C.: South east tropical Atlantic warm events and southern African rainfall. *Geophys. Res. Lett*., **30**, 8009, doi:10.1029./2002GL014840, 2003.

Rouault, M.: Bi-annual intrusion of tropical water in the northern Benguela upwelling. *Geo. Phys. Lett*., **39**, L12606, doi:10.1029/2012GL052099, 2012.

Rouault, M., Illig, S., Lübbecke, J., and Koungue, R. A. I.: Origin, development and

Ocean Sci. Discuss., https://doi.org/10.5194/os-2018-80
Manuscript under review for journal Ocean Sci.
Discussion started: 11 September 2018

demise of the 2010-2011 Benguela Niño. *J Mar. Syst.*, http://dx.doi.org/10.1016/j.jmarsys.2017.07.007, 2017.

Saha S., and Co-authors.: The NCEP Climate Forecast System Reanalysis. *Bull. Ame. Meteoro. Soc.*, doi:10.1175/2010BAMS3001.1, 2010.

Santos, F., Gomez-Gesteria, M., deCastro, M., and Alvarez, I.: Differences in coastal and oceanic SST trends due to the strengthening of coastal upwelling along the Benguela current system. *Continental Shelf Research*, **34**, 79-86, 2012.

Small, R. J., Thomas, R. A., and Bryan, F. O.: Storm track response to Ocean Fronts in a global high-resolution climate model. *Clim. Dyn.*, doi:10.1007/s00382-013-1980-9, 2014.

Stommel, H.: The Gulf Stream: a physical and dynamical description. 2nd ed. University of California Press, Berkley and Cambridge University Press, London, 1965.

Tozuka, T., and Cronin, M. G.: Role of mixed layer depth in surface frontogenesis: The Agulhas Return Current front. *Geophys. Res. Lett.*, doi:10.1002/2014GL059624, 2014

Tozuka, T., Ohishi, S., and Cronin, M. G.: A metric for surface heat flux effect on horizontal sea surface temperature gradients. *Clim. Dyn.*, **51**, 547-561, doi:10.1007/s00382-017-3940-2, 2018.

Veitch, J. A., Florenchie, P., and Shillington, F. A.: Seasonal and interannual fluctuations of the Angola-Benguela Frontal Zone (ABFZ) using 4.5 km

Ocean Sci. Discuss., https://doi.org/10.5194/os-2018-80
Manuscript under review for journal Ocean Sci.
Discussion started: 11 September 2018

resolution satellite imagery from 1982 to 1999. *Int. J. Remote Sens*ing, **27**, 987-998, doi:10.1080/01431160500127914, 2006.

Vizy, E. K., Cook, K. H., and Sun, X.: Decadal change of the south Atlantic ocean Angola-Benguela forntal zone since 1980. *Clim. Dyn.*, https://doi.org/10.1007/s00382-018-4077-7, 2018.

Xu Z., Chang, P., Richter, I., Kim, W., and Tang, G.: Diagnosing southeast tropical Atlantic SST and ocean circulation biases in the CMIP5 ensemble. *Clim. Dyn.*, **43**, 3123-3145, doi:10.1007/s00382-014-2247-9, 2014.

Figures

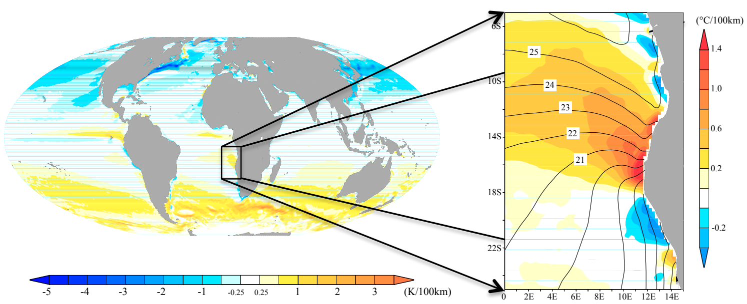

Figure 1.
(Left) Global image of observed annual-mean SST meridional gradient from 1982-2010 of OISST. (Right) annual-mean SST (contour, °C) and its meridional gradient (°C/100km) around the ABFZ.

Ocean Sci. Discuss., https://doi.org/10.5194/os-2018-80
Manuscript under review for journal Ocean Sci.
Discussion started: 11 September 2018

Ocean Science Discussions
Open Access

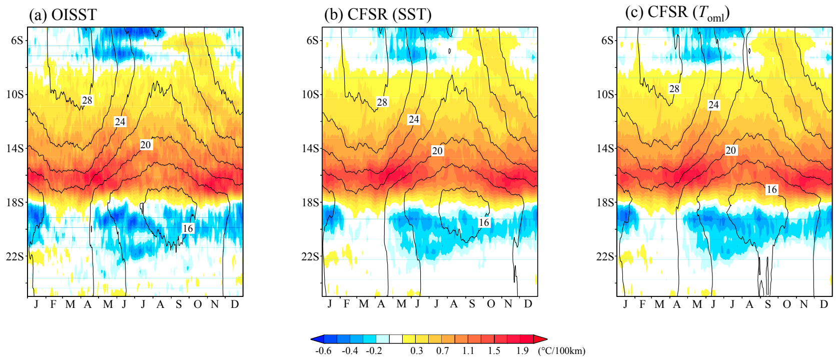

Figure 2.
Climatological seasonal cycle of the temperature (contour) and its meridional gradient averaged between 10°E and 12°E for (a) SST of OISST, (b) SST of CFSR, and (c) OML-mean potential temperature of CFSR.

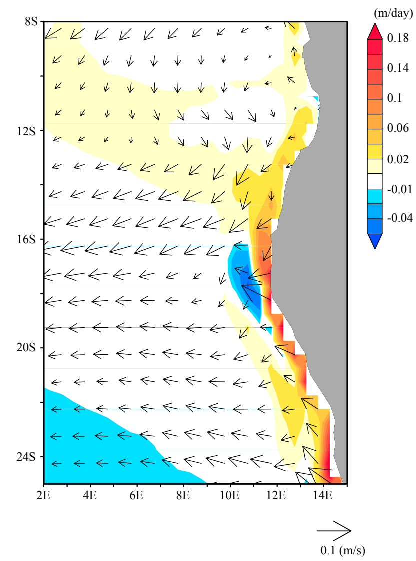

Figure 3.
Annual-mean climatological states of OML-mean horizontal current (arrows) and vertical velocity at the bottom of OML (color).

Ocean Sci. Discuss., https://doi.org/10.5194/os-2018-80
Manuscript under review for journal Ocean Sci.
Discussion started: 11 September 2018

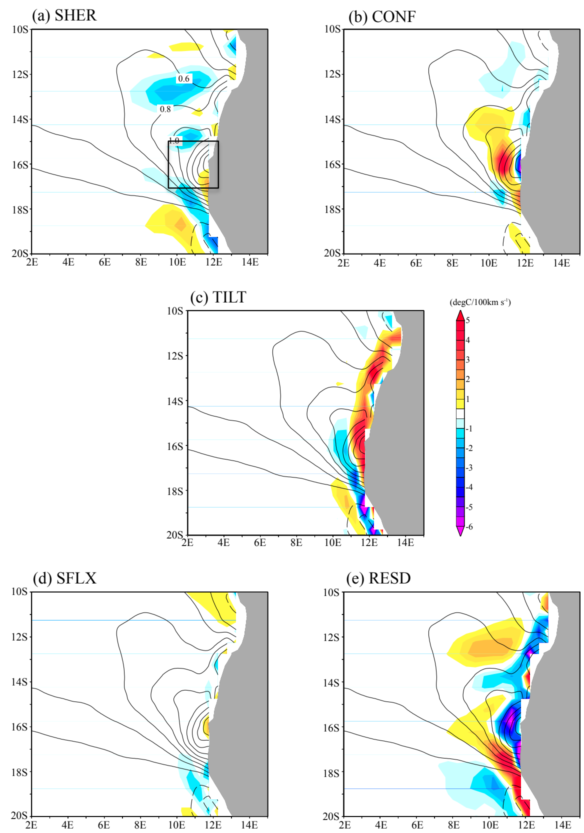

Figure 4.
Annual-mean climatology of each term in OFGF. Contour is annual-mean climatology of meridional gradient of OML-mean potential temperature of CFSR (°C/100km). The black box on (a) is the ABFZ used for the analysis in this study.

Ocean Sci. Discuss., https://doi.org/10.5194/os-2018-80
Manuscript under review for journal Ocean Sci.
Discussion started: 11 September 2018

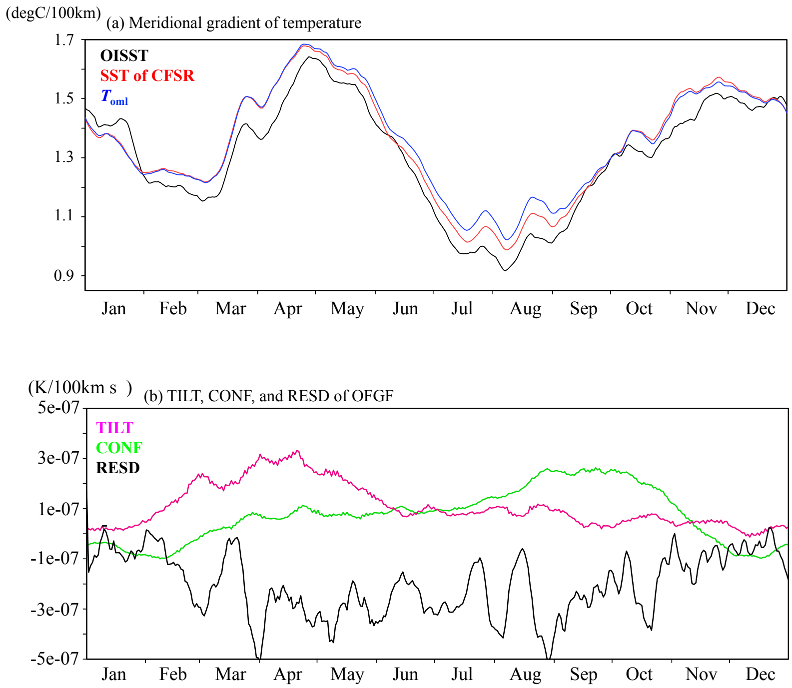

Figure 5.
Box-mean (17°S-15°S and 10°E-12°E) time series of (a) meridional gradient of temperature (black: OISST, red: SST of CFSR, and blue: OML-temperature of CFSR) and (b) TILT (magenta), CONF (green) and RESD (black). 11days-running mean are shown for all the time series.

592

Ocean Sci. Discuss., https://doi.org/10.5194/os-2018-80
Manuscript under review for journal Ocean Sci.
Discussion started: 11 September 2018

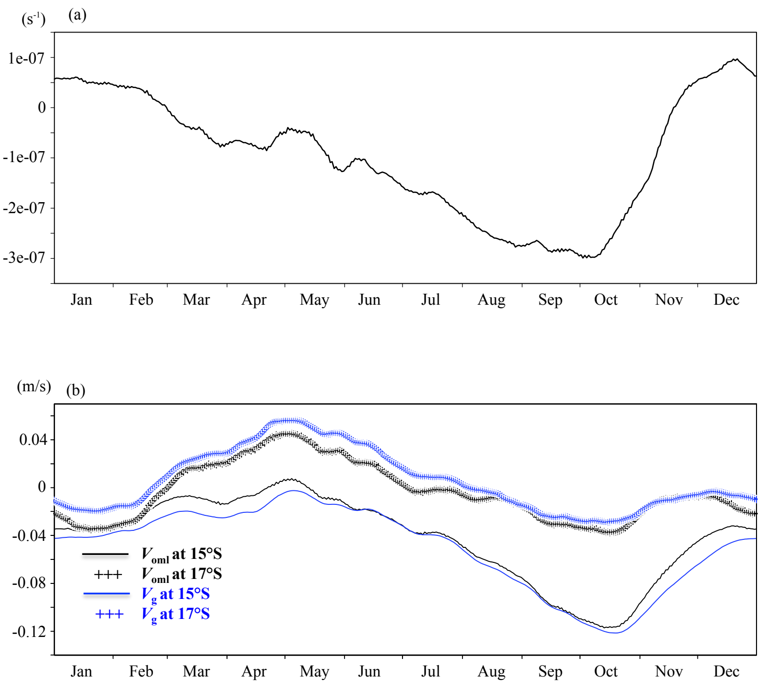

Figure 6.
Time series of (a) $\partial v_{oml} / \partial y$ averaged over (17°S-15°S and 10°E-12°E) and (b) OML-mean meridional current velocity (black) and geostrophic meridional current velocity estimated from sea surface height (blue) at 15°S (solid line) and 17°S (+ mark) averaged between 10°E and 12°E. All variables are filtered by moving 11-days window.

593

Ocean Sci. Discuss., https://doi.org/10.5194/os-2018-80
Manuscript under review for journal Ocean Sci.
Discussion started: 11 September 2018

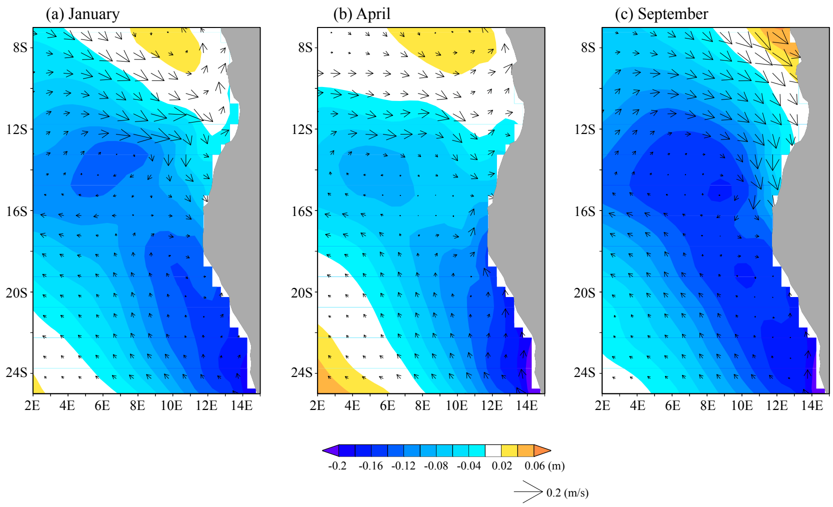

Figure 7.
Monthly mean SSH (color) and geostrophic current (arrows) for (a) January, (b) April, and (c) September.

594

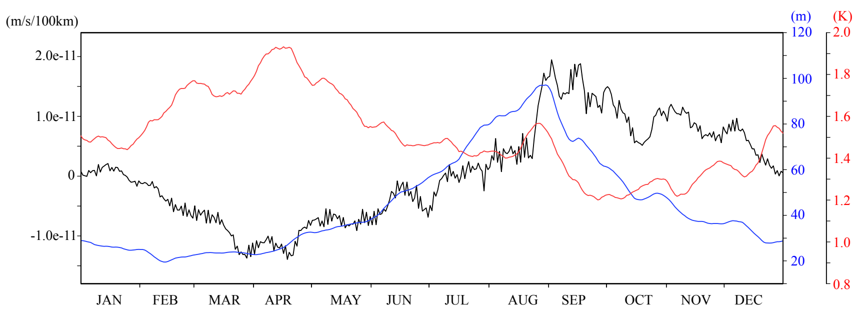

Figure 8. Time series of the area-averaged meridional gradient of the vertical velocity at the bottom of OML (black), OML depth (blue), intensity of upper ocean thermocline stratification (red) over 17°S-15°S and 10°E-12°E. All variables are filtered by moving 11-days window.

595

596